Journal of Molecular Catalysis A: Chemical 398 (2015) 325–335

Contents lists available at ScienceDirect

Journal of Molecular Catalysis A: Chemical

journal homepage: www.elsevier.com/locate/molcata

Superficial effects and catalytic activity of ZrO_2–SO_4^{2-} as a function of the crystal structure

Cristian D. Miranda M.[a,*], Alfonso E. Ramírez S.[a], Sonia Gaona Jurado[b], Carlos R. Vera[c]

[a] Grupo Catálisis, Departamento de Química, Universidad del Cauca, Popayán-Cauca, Calle 5 No. 4-70, Colombia
[b] Grupo CYTEMAC, Departamento de Física, Universidad del Cauca, Popayán-Cauca, Calle 5 No. 4-70, Colombia
[c] Instituto de Investigaciones en Catálisis y Petroquímica- INCAPE (FIQ, UNL- CONICET), Santiago del Estero 2654, 3000 Santa Fe, Argentina

ARTICLE INFO

Article history:
Received 9 March 2014
Received in revised form
19 November 2014
Accepted 21 December 2014
Available online 30 December 2014

Keywords:
Zirconium oxide
Sulfated zirconia
Acid catalysis
Sucrose inversion
Glycerol esterification

ABSTRACT

As assessment was made of the influence of the crystal structure on the activity of SO_4^{2-}–ZrO_2 catalysts for the acid-catalyzed reactions of sucrose inversion and the esterification of fatty acids with glycerol. Purely monoclinic or purely tetragonal SO_4^{2-}–ZrO_2 catalysts were synthesized by sulfation with 1 M sulfuric acid of different ZrO_2 starting materials of defined crystal phase. The final catalysts were obtained by calcination at 400 °C, a relatively mild temperature for this kind of materials. Structural and morphological characterization tests showed that the crystal phase of zirconia had an influence on the properties of the sulfated zirconia catalysts. Monoclinic and tetragonal catalysts had different acidities and also different levels of activity in the reactions. Better results in the sucrose inversion tests were obtained using tetragonal phase catalysts while monoclinic phase materials were better catalysts for glycerol esterification.

The catalysts were further characterized by Fourier transform infrared spectroscopy (FT-IR), X-ray powder diffraction (XRD), transmission electron microscope (TEM), X-ray photoelectron spectroscopy (XPS) and nitrogen physisorption. The acidity was measured by amine titration using Hammett indicators and FT-IR absorption of adsorbed pyridine.

1. Introduction

Sulfated zirconia has been extensively used as a heterogeneous catalyst in many organic reactions [1]. The results show that it is an excellent material for catalyzing reactions that need of strongly acidic active sites [2,3]. The most common synthesis of zirconium hydroxide involves the precipitation from aqueous solutions of zirconium salts ($ZrOCl_2{\cdot}8H_2O$ [4], $ZrCl_4$ [5], $ZrO(NO_3){\cdot}xH_2O$ [6], etc.) with ammonium hydroxide [7,8]. Next the formed precipitate is dried, sulfated with H_2SO_4 or $(NH_4)_2SO_4$, and calcined [4–8]. The sulfate ion produces a preferential stabilization of the tetragonal phase during calcination of the sulfated Zr hydroxide gel, the growth of the monoclinic phase being highly inhibited. This stabilization of the tetragonal phase precludes a clear elucidation of the relationship between the catalytic activity and the specific crystal phase of this kind of catalysts. One way to circumvent this problem is to work with catalysts synthesized by sulfation of crystalline zirconia supports. Studies on these type of catalysts have led some authors to propose that the tetragonal phase stabilization is a consequence of the relation between crystal defects and the metastable tetragonal phase [9]. Zirconia can be found in one of three different crystalline forms: monoclinic (*M*), stable at temperatures below 1100 °C; tetragonal (*T*), stable at temperatures between 1100–1900 °C; and cubic (*C*), stable at temperatures above 1900 °C. The *T* and *C* structures can however be obtained and maintained as a metastable structure at lower temperatures [10]. In the case of sulfated zirconia catalysts the final crystal structure is a function of the activation temperature [11], the sulfation process [12], and the presence of dopants [13]. Generally speaking, catalysts crystallized in the tetragonal phase usually display the higher catalytic activity [13–15]. However, sulfated zirconia catalysts with monoclinic crystal phase also have catalytic activity and meaningful levels of surface acidity [16]. In this sense, several authors believe that sulfated zirconia with "superacid" properties cannot be obtained by sulfation of crystalline monoclinic zirconia and that it is necessary to sulfate amorphous precursors, especially Zr hydroxide[17].

In this paper, we present results related to the preparation of sulfated zirconia catalysts with monoclinic and tetragonal phase,

* Corresponding author. Tel.: +57 8217027.
E-mail address: cdmiranda@unicauca.edu.co (C.D. Miranda M.).

http://dx.doi.org/10.1016/j.molcata.2014.12.015
1381-1169/

their physicochemical characterization and their use in two reactions of interest: the inversion of sucrose and the esterification of glycerol. The synthesis of purely monoclinic or purely tetragonal catalysts is performed by sulfation of crystalline supports. The final catalysts were obtained by calcination at 400 °C, a relatively mild temperature for this kind of catalysts, that seemingly enabled the stabilization of a high concentration of surface sulfates. The obtained catalysts had a lower acid strength than that reported for classical sulfated zirconia catalysts obtained by impregnation of the amorphous support. The lack of "superacid" properties and the presence of "mild" acid sites permitted the catalysis of the proposed reactions with good selectivity due to the absence of very strong acid sites catalyzing oligomerization and cracking. The influence of the crystal phase on the resulting physical and catalytic properties is thus assessed and discussed.

2. Experimental

2.1. Catalysts preparation

2.1.1. Tetragonal zirconium oxide

The synthesis of this material was performed following the technique of Rodríguez and Campo [18]. The precursors were zirconium oxychloride ($ZrOCl_2{\cdot}8H_2O$, Merck 99%) and calcium acetate ($Ca[CH_3COO]_2$, Carlo Erba 99,9%). Two different solutions of the salts were precipitated independently with ammonium hydroxide (NH_4OH, Mallinckrodt 28%) at 60 °C. After aging for 24 h the resulting slurries were thoroughly mixed and then filtered. The filtered gel was then washed with a 0.01 M diethylamine solution and dried at 80 °C for 48 h. The support was finally calcined at 600 °C for 1 h.

2.1.2. Monoclinic zirconium oxide

The synthesis process was the same one used for the tetragonal sample. Zirconium oxychloride was also used as precursor but no calcium acetate was added and the precipitated gel was calcined at 400 °C.

2.1.3. Sulfated zirconia catalysts

The method of immersion was used for sulfating the zirconia supports. The samples were dipped (15 mL g^{-1} of catalyst) [19] in a 1 M H_2SO_4 solution for 30 min. The solution was stirred gently with a magnetic bar and kept at 50 °C. The final solid was then filtered in vacuum and dried overnight at 100 °C in a stove. The material was finally calcined at 400 °C in air (200 mL min^{-1}, 2 h).

2.2. Characterization

The monoclinic and tetragonal zirconia unsulfated supports and the sulfated catalysts were both characterized by Fourier transform infrared (FT-IR) spectroscopy in order to verify the effective sulfation of zirconia by the appearance of the band in the range of 990–1250 cm^{-1}. This is a band characteristic of sulfate groups bound to the zirconia oxide [20]. Spectra were collected using an FTIR Thermo Nicolet IR200 spectrometer in the 4000–400 cm^{-1} range.

The samples were also studied by XRD in order to determine their crystallinity and crystal structure and to determine the influence of sulfation. They were ground to a powder and analyzed in a PANalytical X'Pert Pro X-ray diffractometer using Cu-Kα radiation (λ = 1.5405 Å). The spanned range was 2θ = 5–90° and the scan rate was 2° min^{-1}.

The morphology of sulfated zirconia was determined by transmission electronic microscopy (TEM) with a JEOL 1200 EX electronic microscopy operated at an accelerating voltage of 80 kV. The samples were prepared by covering 100 mesh copper grids with 10 mg of the zirconia powders (either sulfate doped or sulfate free).

The surface chemical composition was determined by X-ray photoelectron spectroscopy (XPS) in a Surface Science Instruments S-Probe (VG) equipment, using Al Kα radiation (1486.6 eV).

The surface area of the samples was measured by nitrogen physisorption at −196 °C in a Micromeritics Tristar 3000 equipment. The specific surface area was determined from the isotherm data by using the BET equation.

2.2.1. Acid strength measurements

The acid strength was determined by means of the Hammett indicator method. Color tests were made by transferring 0.1 g of the samples in powder form to a test tube and then adding three drops a 0.1% solution of indicator dissolved in benzene. The samples were first dried at 120 °C before carrying out the indicator tests. The color test was performed immediately after taking the samples from the stove.

The amount of acid sites on the samples was measured by the amine titration method. A 0.1 N titrating solution was prepared by weighing 1.0 mL of *n*-butylamine in a 100 mL volumetric flask and making up the volume using dried benzene. The titrating procedure was as follows: 0.2 g of the dried sample were transferred to a 50 mL screw cap Erlenmeyer flask. 9 mL of dry benzene and 3 mL of the indicator solution in benzene were added to the sample suspension. Then the titrating solution was added from a 2 mL burette to the sample so as to bracket the expected titer by the appropriate number of millimoles of *n*-butylamine per gram of sample. The titration was then continued using smaller stepwise increases in *n*-butylamine content until the end point.

The surface acidity of the solid catalyst was assessed by measuring the infrared absorption of adsorbed pyridine in a Nicolet Nexus FT-IR spectrometer. The samples were pressed into thin wafers (10–20 mg cm^{-2}) and pretreated in an IR quartz cell under secondary vacuum (10^{-6} mbar) at 450 °C for 3 h (fresh sample). After the pretreatment the samples were cooled down to 150 °C and contacted with pyridine vapors (P_{eq} = 2–3 mbar) for 10 min. Then the pyridine excess was removed for 1 h under secondary vacuum and the IR spectra were recorded. The values of concentration of Brønsted and Lewis sites able to retain the pyridine at 150–450 °C were determined by integrating the areas of the bands at 1541 and 1454 cm^{-1}, respectively.

2.3. Catalytic studies

2.3.1. Sucrose inversion reaction

The reaction tests were performed in a batch reactor at 620 kPa in nitrogen, 90 °C and 1000 rpm of stirring rate. In each test 50 mL of a 0.01 M sucrose solution and 0.2 g of catalyst were put in the reactor. A water:ethanol (50–50) solution was used as solvent. The reaction time was 7 h for all tests.

The reaction products were analyzed by HPLC in a Hewlett Packard 1100 liquid chromatograph equipped with a Phenomenex column (150 m, 4.60 mm ID, 5 μm film thickness) and a UV–vis detector. The mobile phase was 70:30 acetonitrile-water and was pumped at 0.5 mL min^{-1}. Samples of 0.0025 μL were used. The reactants and products were identified by comparison of the experimental elution peaks with those produced by commercial standards.

2.3.2. Glycerol esterification

The esterification reaction was performed in a glass batch reactor equipped with a condenser. The glycerol (1.0 g) and the fatty acid (2.2 g) (molar ratio of glycerol to fatty acid equal to one) were stirred at 800 rpm and heated on a hot plate at the required temperature (100 °C generally). When the desired temperature was

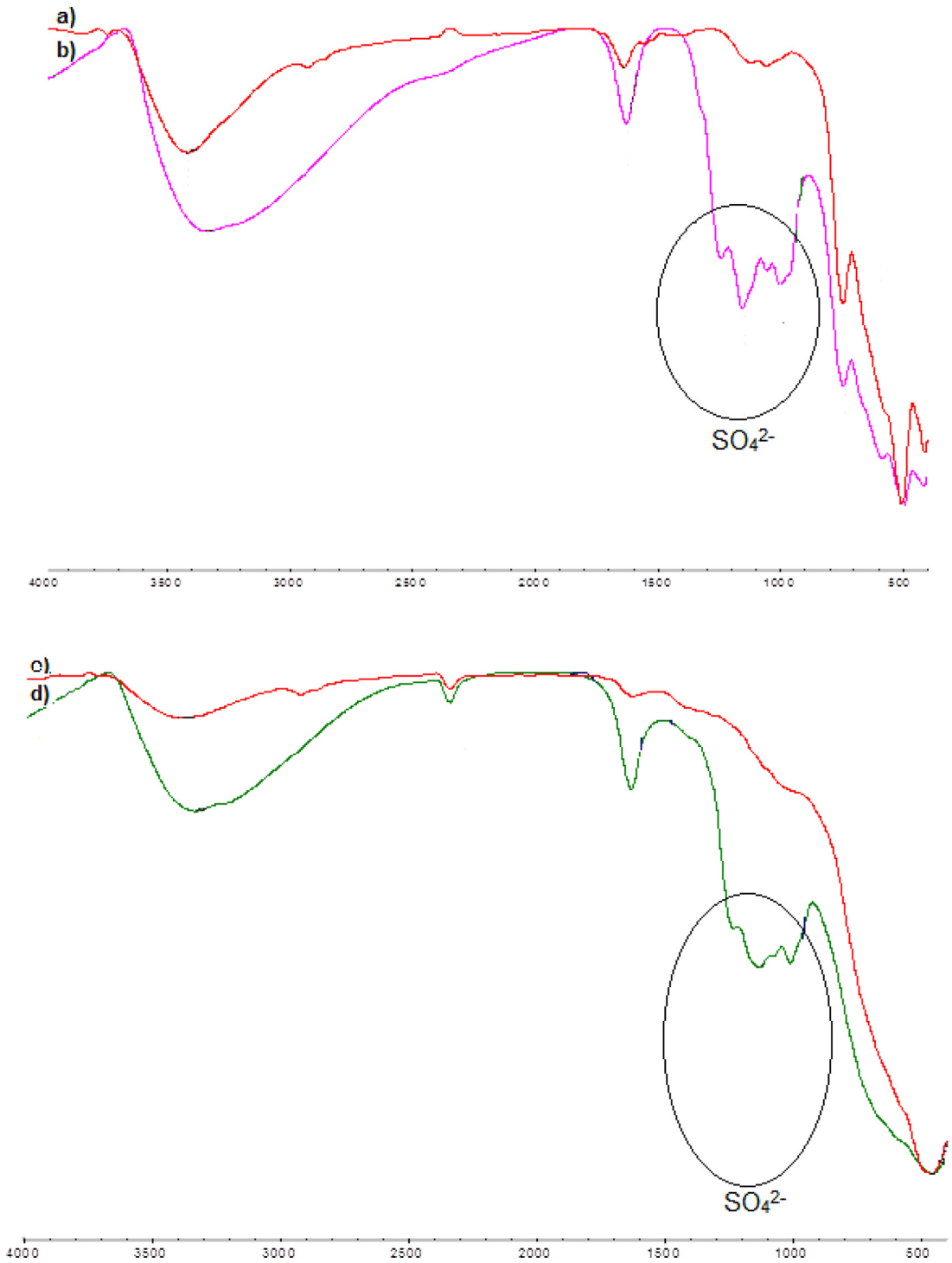

Fig. 1. FT-IR spectra of the sulfate-free and sulfate-doped zirconia samples. (a) Monoclinic ZrO_2, (b) Monoclinic ZrO_2–SO_4^{2-}, (c) Tetragonal ZrO_2, (d) Tetragonal ZrO_2–SO_4^{2-}.

reached, the catalyst (0.16 g) was added to the reactor (zero reaction time). After cooling down the reaction products (after about 15 min), ethanol (5 mL) was added in order to make the products solution more homogeneous and a sample was taken for analysis by gas chromatography.

The products were analyzed by gas chromatography in a Shimadzu GC-14A chromatograph equipped with a flame ionization detector and a Restek RTX-5 (30 m, 0.32 mm ID, 0.25 μm film thickness) capillary column. Dodecane (99%, Acros Organics) was used as an internal standard and the chromatograms were processed in a Shimadzu CR-15A integrator connected online.

3. Results and discussion

3.1. Sulfation method assessment

3.1.1. IR spectroscopy

A first assessment of the amount and kind of sulfate groups (SO_4^{2-}) in the final catalysts was made by infrared spectroscopy.

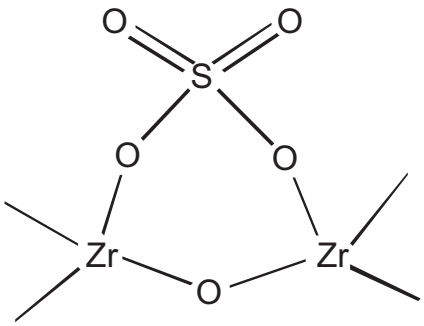

Fig. 2. Bidentate bridging structure of surface sulfate ion bound to zirconium oxide [20].

Fig. 1 shows the infrared spectra of the monoclinic ZrO_2 sulfate-free sample (Fig. 1a) and of the same samples after being sulfated (Fig. 1b). Similarly Fig. 1c shows the infrared spectrum of the unsulfated tetragonal zirconia sample and Fig. 1d the spectrum of the sulfated tetragonal zirconia catalyst.

The bands at 1000, 1063, 1149 and 1242 cm^{-1}can only be detected on the sulfate-doped samples. They are associated to vibrations of the sulfate ion bound to surface Zr atoms indicating an effective sulfation of the surface of zirconium oxide. Moreover, the position of these bands suggests that the binding between Zr and sulfate is through a bidentate bridging ligand [20] (see Fig. 2).

3.1.2. X-ray photoelectron spectroscopy

In order to know how the sulfate species enhances the surface acidity of zirconia some samples were probed using X-ray photoelectron spectroscopy (XPS). Fig. 3 shows the XPS spectra of the monoclinic samples. As shown in Fig. 3a for the unsulfated sample, two states of oxygen are readily resolved by XPS with O 1s binding energies at 530.0 and 530.5 eV. The first one corresponds to Zr—O and the second one to oxygens of surface OH groups [21]. In the case of the sulfated monoclinic sample, its XPS spectrum (Fig. 3b) has a new signal at 534.1 eV, that is an indication of oxygen atoms with a different chemical environment, such as the oxygens of the sulfate groups SO_4^{2-} [22].

Fig. 4 shows the XPS spectra of the tetragonal ZrO_2 samples. In the case of the unsulfated sample (Fig. 4a) the spectrum has strong signals at 529.1 and 530.6 eV, similar to those found in the spectrum of monoclinic zirconia. Also both monoclinic and tetragonal zirconia had doublets at 182.0 and 184.5 eV, corresponding to the binding energy of Zr 3d in the oxidation state IV [23]. The spectrum of the sulfated tetragonal sample (Fig. 4b) has a new signal at 532.2 eV. As in the case of the monoclinic samples, this is again attributed to the presence of oxygen atoms in sulfate groups. The Zr region also has some differences in comparison to the same spectrum zone of the unsulfated sample. According to Ardizzone [23], these bands are characteristic of zirconia after being treated with sulfuric acid (H_2SO_4), with components at 182.8 eV in Fig. 3b (monoclinic sample) and 183.3–186 eV in Fig. 4b (tetragonal sample) corresponding to Zr (IV) linked to electron-attractive groups. The spectra of both the monoclinic and tetragonal samples have a wide range of values in the Zr 3d region, that according to literature reports [24] would be typical of the IV oxidation state of Zr.

With respect to the presence of sulfur on the surface after the sulfation process, there is a band that corresponds to the S 2p level. In sulfated zirconia, either monoclinic or tetragonal, this band is divided into two components at 169 and 170 eV. The difference between both values is possible due to the protonation of sulfate: species located around 169 eV would correspond to deprotonated sulfated species whereas those located at around 170 eV would be protonated sulfated species [24]. Mainly deprotonated sulfate

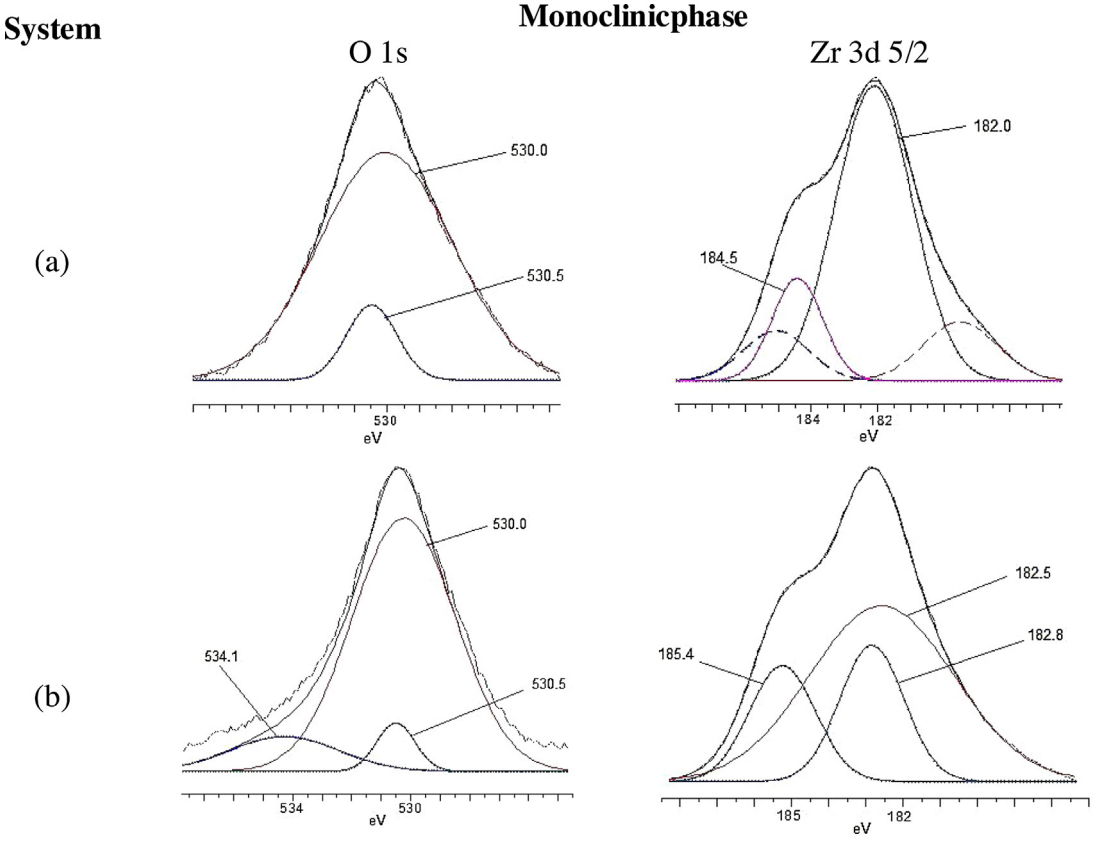

Fig. 3. XPS spectra of monoclinic zirconia: (a) ZrO_2, (b) ZrO_2–SO_4^{-2}.

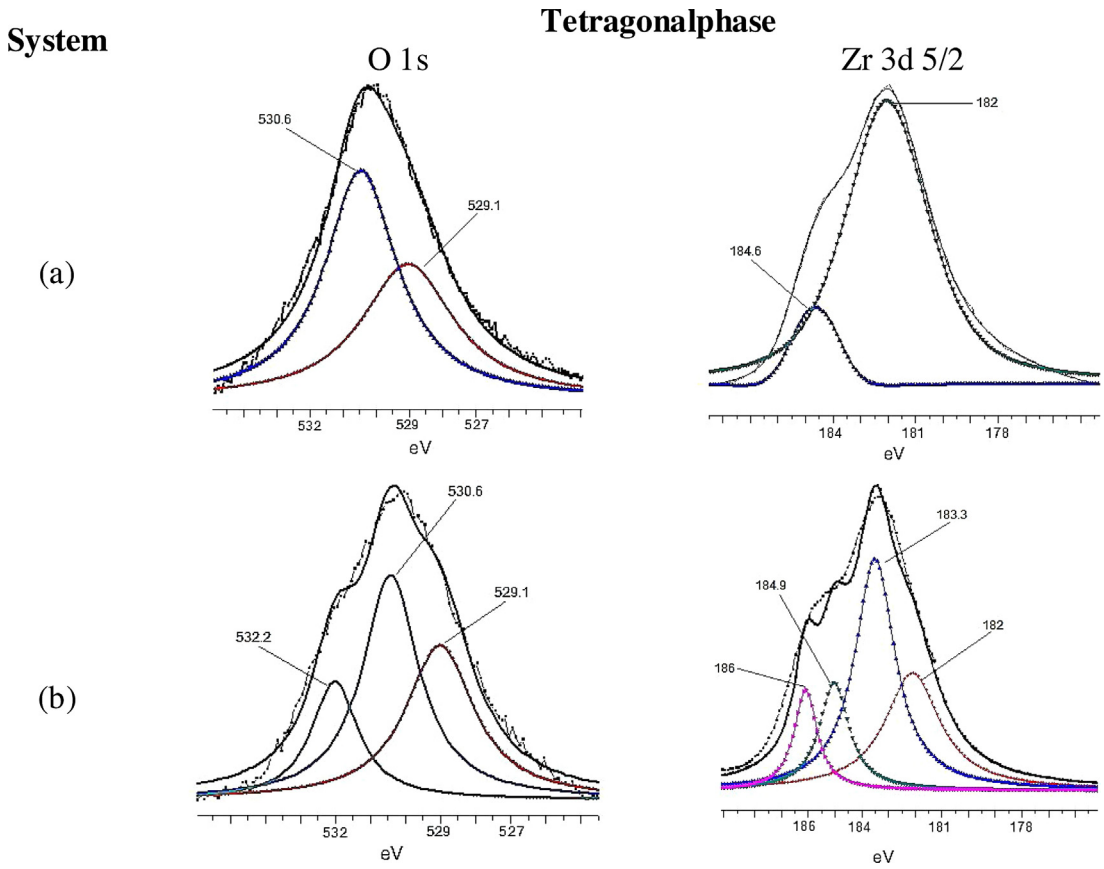

Fig. 4. XPS spectra of tetragonal zirconia: (a) ZrO_2, (b) ZrO_2–SO_4^{-2}.

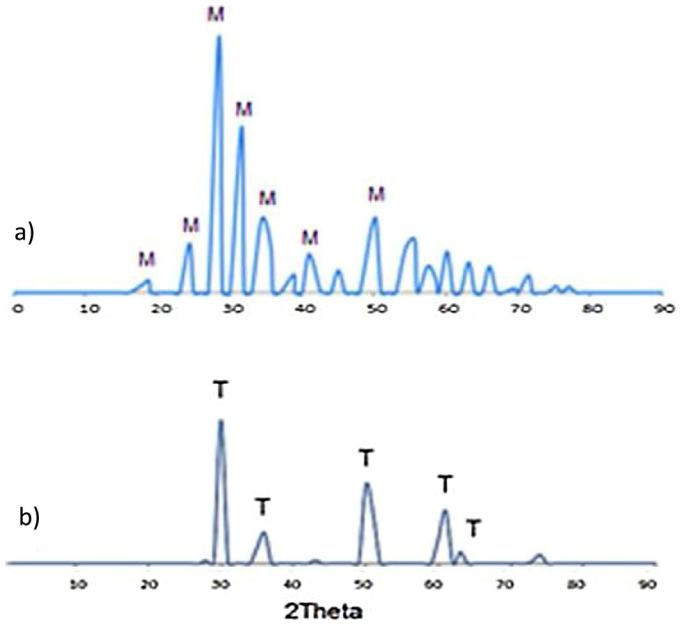

Fig. 5. X-ray diffractograms. (a) Monoclinic unsulfated zirconia (M) and (b) tetragonal unsulfated zirconia (T).

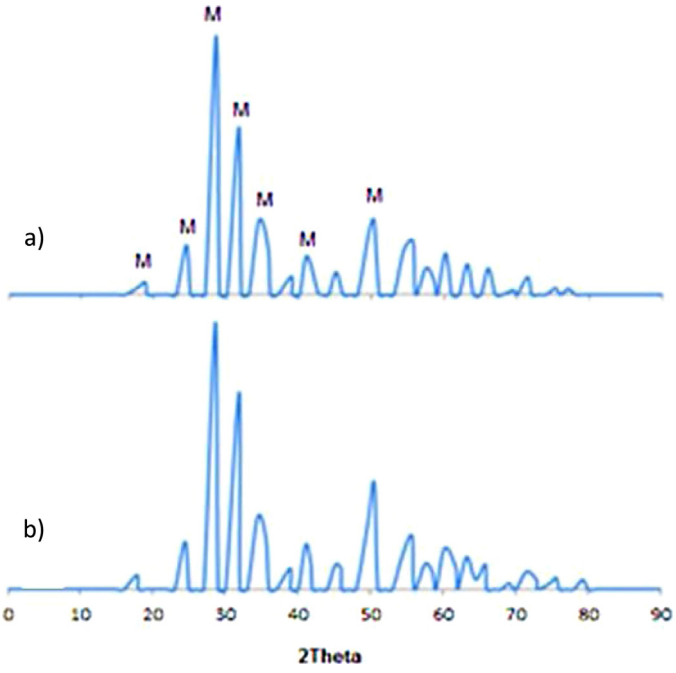

Fig. 6. Influence of sulfation on the crystal structure of monoclinic ZrO_2. (a) Sample without sulfation, (b) sample after sulfation and calcination.

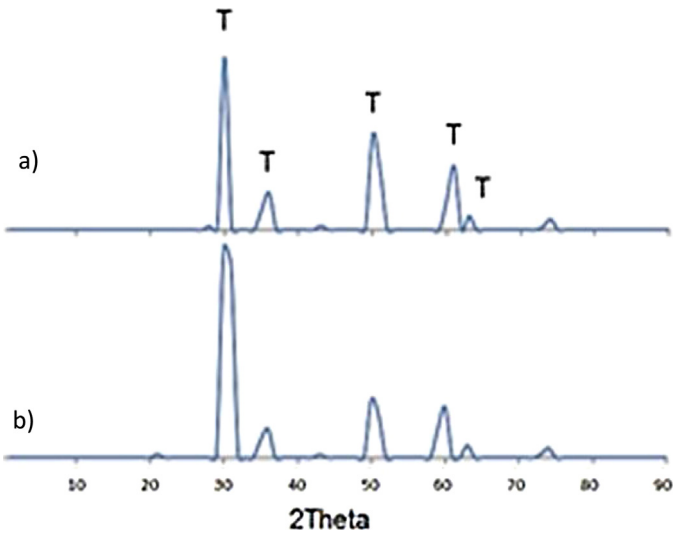

Fig. 7. X-ray diffraction patterns of tetragonal ZrO_2. (a) Without sulfation, (b) after sulfation with 1 M H_2SO_4 and calcination.

species can be seen in our results. This is agreement with the observed bridging bidentate complex detected in the IR analysis.

3.2. Morphological and superficial effects of sulfation process

3.2.1. X-day diffraction

Fig. 5 contains the X-ray diffractograms of the unsulfated zirconia samples. These diffractograms coincide with those published for the monoclinic (PDF 37-1484) and tetragonal (PDF 88-1007) zirconia phases [25].

Fig. 6 shows the X-ray diffractograms of the monoclinic sample before and after sulfation. A comparison of the two diffractograms indicates that there are practically no changes. This means that the treatment of sulfation and subsequent calcination does not produce any change of the crystal structure.

The same stability of the crystal phase can be seen in the case of the tetragonal phase. The results of Fig. 7 indicate that no changes in the XRD peaks or the crystallinity of the tetragonal zirconia sample occur due to the sulfate promotion.

An inspection to the spatial coordination of Zr in the monoclinic and tetragonal zirconia phases (Fig. 8) reveals that Zr is surrounded by 7 oxygen atoms in monoclinic zirconia and by 8 in tetragonal zirconia [26]. This difference would make the monoclinic phase more amenable to surface sulfation, because the Zr is less shielded by oxygen atoms and the incoming sulfate anion finds less electrostatic repulsion from negative oxygen anions.

3.2.2. Transmission electron microscopy

The monoclinic and tetragonal zirconia samples had different morphological features too. Fig. 9 contains TEM micrographs of the unsulfated monoclinic and tetragonal samples. Both have particles of semispherical shape but they have different size. The mean diameter of the monoclinic zirconia particles is about 30 nm while the mean diameter of the tetragonal particles is about 200 nm.

Fig. 10 shows TEM micrographs of the zirconia samples after the sulfation treatment. As anticipated by the XRD results, no changes in the morphology can be detected. Both the monoclinic and zirconia samples retain their semispherical shape and their original size.

3.2.3. Nitrogen adsorption results

Table 1 shows the results of nitrogen physical adsorption of the zirconia samples. Both the tetragonal and monoclinic samples had small values of specific surface area, as measured by the BET method.

Table 1
Specific surface area of the zirconia samples.

Sample	S_{BET} (m^2/g)
Monoclinic	
ZrO_2	19.6
ZrO_2–SO_4^{-2} 1M	22.2
ZrO_2–SO_4^{-2} 6M	11.8
Tetragonal	
ZrO_2	8.6
ZrO_2–SO_4^{-2} 1 M	11.2
ZrO_2–SO_4^{-2} 6M	7.9

Tetragonal zirconia had 8.6 $m^2\,g^{-1}$ while monoclinic zirconia had 19.6 $m^2\,g^{-1}$. The small values of surface area are typical of samples of zirconia without textural promoters subjected to calcination. Sulfate promotion of amorphous zirconia gels results not only in the stabilization of the tetragonal phase but also in a delay of sintering and crystallization phenomena thus leading to samples with high values of surface area, normally in excess of 100 $m^2\,g^{-1}$ for samples calcined at 500–600 °C. Without sulfate the gel crystallizes at normal temperatures and the heat treatment results in a higher crystal growth. This is evident in the X-ray diffractograms of the previous sections, that had well defined peaks with a high height-to-width ratio.

The lower specific surface area of the tetragonal sample is most probably a consequence of the higher calcination temperatures employed for its synthesis. The monoclinic sample was calcined at 400 °C before sulfation and tetragonal zirconia at 600 °C. Both samples were again calcined at 400 °C after sulfation.

The sulfation treatment had a different effect depending on the concentration of the sulfuric acid solution. In the case of the 1 M solution, a small increase in surface area is detected upon sulfation. This could be the result of the acid etching of the surface that results in the formation of grooves and notches. These surface irregularities would increase the surface area [27]. A treatment with solutions of higher concentration would result in dissolution of zirconia and collapse of the pore structure. This would explain the results for the samples treated with 6 M H_2SO_4, that displayed the smallest area values. The existence of an optimum concentration of H_2SO_4 has previously been reported for the case of the sulfation of freshly precipitated gels [28].

3.3. Surface acidity

3.3.1. Amine titration using Hammett indicators

Results on the strength and the amount of acid sites of the zirconia samples are given in Table 2. The limits of the H_0 of the samples were established by observing the color of the adsorbed form of the Hammett indicators [29]. As it can be seen in Table 2

Table 2
Measurement of acid strength by means of Hammett indicators. Unsulfated and sulfated (1 M) zirconia samples.

Indicator		mmol H+/g catalyst			
	pk_a	Monoclinic phase		Tetragonal phase	
		ZrO_2	1 M	ZrO_2	1 M
Neutral red	+6.8	0.2	0.75	0.15	0.55
Methyl red	+4.8	–	0.55	–	0.4
Thymol blue	+1.6	–	0.22	–	0.15
4-Nitroaniline	+1.1	–	0.2	–	0.1
Crystal violet	+0.8	–	0.15	–	0.05
Bromocresol green	−3.7	–	–	–	–
Total	–	0.2	1.87	0.15	1.25

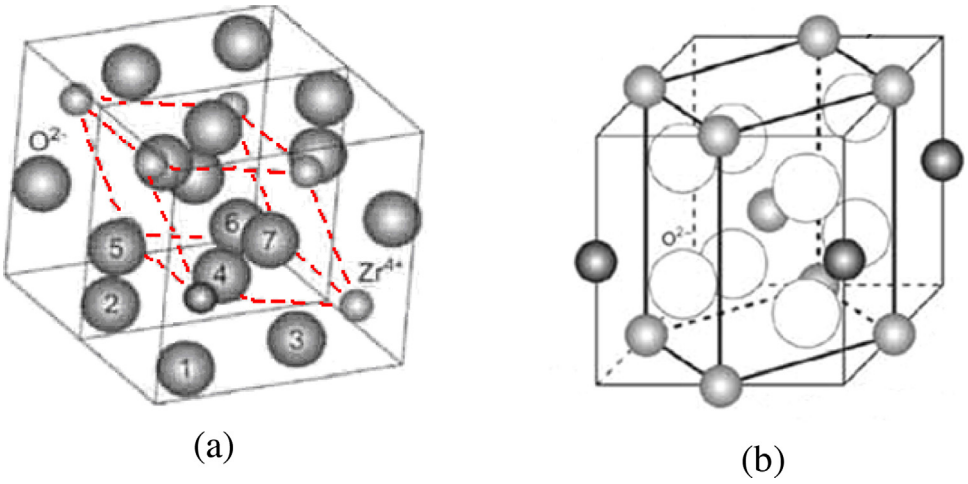

Fig. 8. Coordination of the Zr atom in different crystal phases of ZrO_2. (a) Tetragonal, (b) monoclinic.

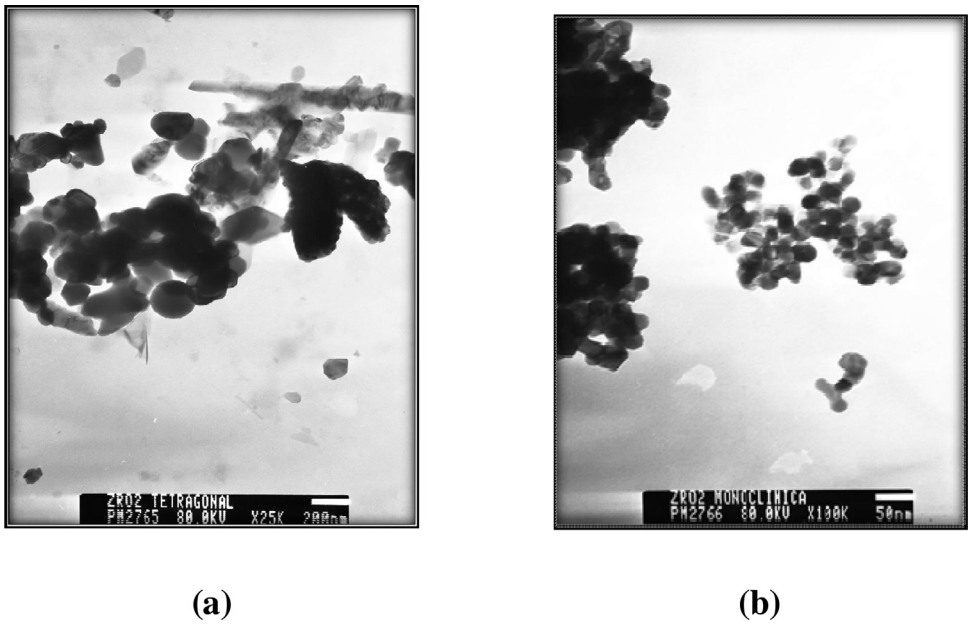

Fig. 9. TEM micrographs of the unsulfated tetragonal (a) and monoclinic, (b) samples.

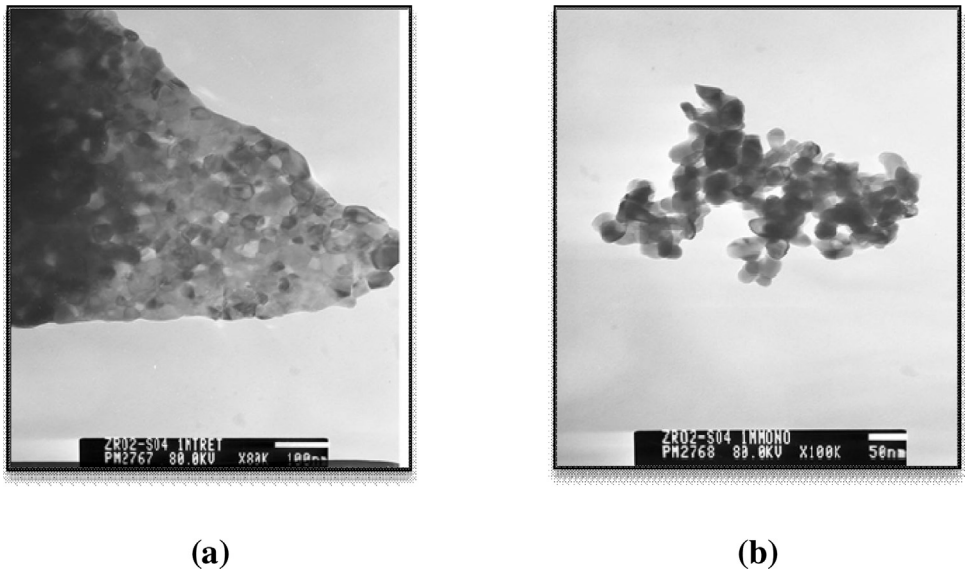

Fig. 10. TEM micrographs of the sulfate promoted tetragonal (a) and monoclinic (b) samples.

Table 3
Concentration and strength of acid sites (in μmol g^{-1}) as calculated from adsorption/desorption of pyridine followed by IR absorption spectroscopy. L = Lewis, B = Brønsted.

T (K)	ZrO_2 Monoclinic		ZrO_2–SO_4^{-2} Monoclinic 1M		ZrO_2 Tetragonal		ZrO_2–SO_4^{-2} Tetragonal 1M	
	L	B	L	B	L	B	L	B
423	71	–	51	5	9	–	11	23
523	21	–	24	4	1	–	4	13
623	2	–	7	–	–	–	1	7
723	2	–	4	–	–	–	–	1

the unsulfated zirconia samples had a similar value of acid strength, $H_0 \leq +2.8$, but a different amount of acid sites, 0.15 mmol g^{-1} (T) and 0.20 mmol g^{-1} (M). It could be argued that the difference in amount of acid sites could be the result of the different surface area, that was bigger for the monoclinic sample. In this sense the calculation of the amount of acid sites per unit area yields 0.017 mmol m^{-2} for the tetragonal sample and 0.010 mmol m^{-2}. Therefore the surface acidity per unit area is indeed higher for the tetragonal sample. A similar reasoning can be made in the case of the sulfated samples. The sulfated monoclinic sample has a higher acidity per unit mass but a lower acidity per unit area (Monoclinic: 1.87 mmol g^{-1}, 0.084 mmol m^{-2}; Tetragonal: 1.25 mmol g^{-1}, 0.112 mmol m^{-2}).

The valid acidity comparison should be that one based on the concentration of acid sites per unit area (a_S, in mmol m^{-2}) because is directly related to chemical properties and independent of the available surface area. As we saw $a_S{}^T$ was higher than $a_S{}^M$. a_S should be the result of the polarizing effect of the electronegative sulfate group. The method of sulfation used an excess of sulfating agent (immersion method) and the calcination temperature was the same for both samples, monoclinic and tetragonal. In this sense the higher value of $a_S{}^T$ can be thought to be due to two different situations: (i) a greater stabilization of sulfate groups on the tetragonal sample, leading to higher values of sulfate groups per unit area; (ii) similar values of the surface concentration of sulfate on both the monoclinic and tetragonal samples; but a higher proportion of acid sites per unit sulfate in the case of the tetragonal sample.

The data of acid strength distribution indicate that this is similar for both sulfated catalysts. Most acid sites (>60%) had pK_a values equal or higher than 4.8 while the most acidic sites had pK_a values higher than −3.7. It can be seen that the strength of the most acidic sites is smaller than that reported for samples of highly acidic sulfated zirconia prepared in the standard way (sulfation of the $Zr(OH)_4$ gel in the amorphous state and calcination at 600–650 °C), that could have sites with pK_a equal to −11.4 in the Hammett scale.

3.3.2. FT-IR study of pyridine adsorption

The results of FT-IR absorption of adsorbed pyridine are presented in Fig. 11. From the obtained spectra, the types of sites affecting adsorption were classified as Lewis (L) or Brønsted (B). The pyridinium ion alone produced a band in the vicinity of 1542 cm^{-1} and the appearance of this band in the spectrum was taken as indication of Brønsted acidity. Pyridine coordinatively bonded on Lewis sites generated a unique band at 1448 cm^{-1} where the pyridinium ion did not absorb. Pyridine itself gave a band at 1440 cm^{-1}.

The IR spectra of samples before and after pyridine adsorption followed by evacuation at successively higher temperatures (150–450 °C) are shown in Fig. 12.

The concentrations of Brønsted and Lewis sites were estimated from the intensities of the bands at 1542 and 1448 cm^{-1} corresponding to the pyridiniumion (Py-H^+) and to pyridine coordinated over Lewis sites (Py-L), respectively. The resulting data is compiled in Table 3. The values obtained show differences between the two phases. In the case of the unsulfated catalysts none of them had Bronsted acid sites or its concentration was negligible. This

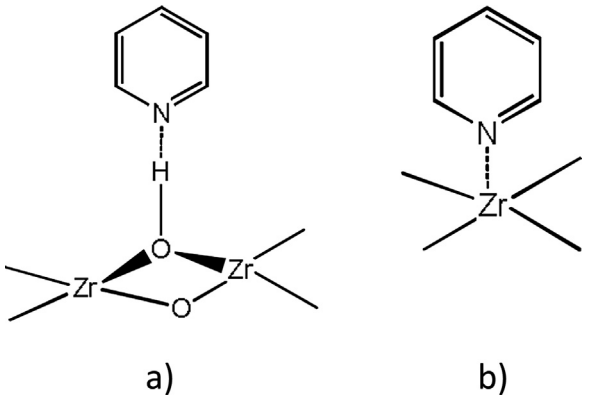

Fig. 11. Species formed during pyridine adsorption. (a) Pyridinium ion (Brønsted site), (b) coordinately bonded pyridine (Lewis site).

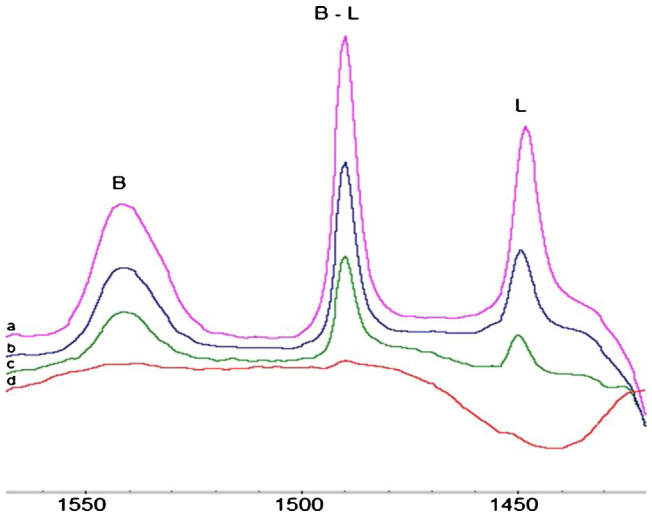

Fig. 12. FTIR spectra of pyridine adsorbed on tetragonal ZrO_2–SO_4^{-2} and evacuated at different temperatures: (a) 150 °C, (b) 250 °C, (c) 350 °C, (d) 450 °C.

was expected since extensive dehydroxylation (loss of surface OH groups) would occur on the sulfate-free zirconia gels during calcination. With respect to the Lewis sites, monoclinic zirconia had almost 8 times the amount of Lewis sites of the tetragonal sample. This could be related to the 7-fold bulk coordination of the Zr atom in monoclinic zirconia (as compared to the 8-fold coordination of Zr in tetragonal zirconia), that might lead to a higher concentration of coordinately unsaturated cations on the surface of the particle. The lower number of oxygen atoms in the sphere of coordination of Zr in monoclinic zirconia could also lead to a higher electron affinity of the Zr^{4+} cation. In this sense some of these Lewis sites on the monoclinic unsulfated sample were of high acid strength and could not be desorbed at the highest temperature, 450 °C. In the case of the tetragonal zirconia sample, all Lewis sites had desorbed pyridine at 350 °C.

When we analyze the results of the sulfated samples some points seem clear: (i) Sulfation only slightly increases the amount of Lewis sites of the unsulfated surface; in this sense most Lewis sites must be those present on the surface before the sulfation treatment and their acid strength seems not be affected by sulfation (range of thermal desorption practically not modified by sulfation). (ii) As acidity is concerned the main role of the sulfate group is to generate new Brønsted acid sites; in this sense this occurs to a greater extent in the case of the tetragonal sample. The Brønsted acid sites generated on the zirconia sample are more numerous and more strong than those generated on the monoclinic sample. No pyridine remains on the monoclinic sample at 350 °C while a non negligible amount is retained on the tetragonal sample at 450 °C.

The mass concentration of 23 μmol g^{-1} Brønsted on tetragonal ZrO_2/SO_4^{2-} translates to about 0.6 sites per square nanometer if the specific surface area of this material is considered. This is a relatively high surface density of acid sites. This could be related to a relatively high concentration of surface sulfates remaining after calcination. It must be recalled that common ZrO_2–SO_4^{2-} catalysts are calcined at 500–600 °C and at this temperature a great portion of the original sulfates present in the freshly impregnated catalyst are lost by thermal decomposition. In this sense the mild calcination temperature employed in our case (400 °C) could have led to a relatively high surface concentration of sulfate and related Brønsted acid groups.

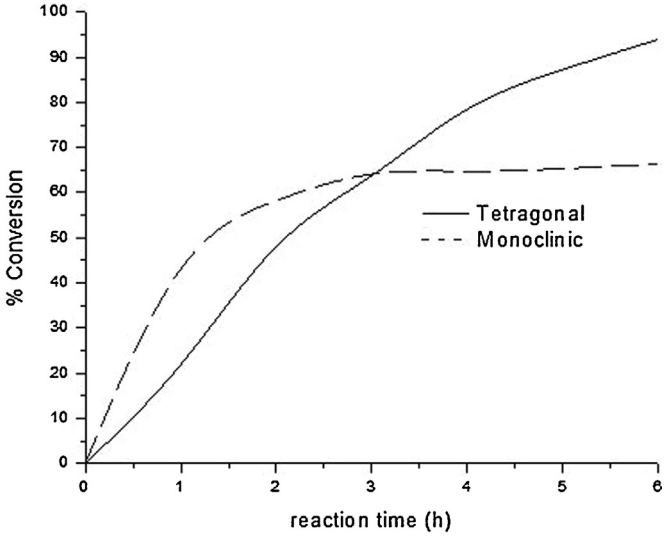

Fig. 13. Conversion of sucrose as a function of reaction time.Sucrose inversion reaction using monoclinic (dashed line) and tetragonal (continuous line) ZrO_2–SO_4^{2-} catalysts. Reaction step conditions: 50 mL of a 0.01 M sucrose solution, 0.2 g of catalyst; 620 kPa in nitrogen, 90 °C, 1000 rpm of stirring rate and 7 h. A water:ethanol (50–50) solution was used as solvent.

3.4. Catalytic evaluation

There was a concern over the probable leaching of sulfate from the catalyst during the reactions. A direct measurement of sulfate in the solid was not done but some additional tests were performed to check the occurrence of sulfate leaching into the reaction media. The tests comprised measuring the concentration of sulfate in the reaction media before and after the reactions by means of the spectrophotometric method (EPA method 375.4). This test was chosen because it involves the use of water and alcoholic solutions as those used in the reactions. Though some catalysts fines were indeed formed after 7 h reaction time, the filtrated solution contained no dissolved sulfate, at least in concentrations higher than the detection limit of the method (1 mg L^{-1}).

3.4.1. Inversion reaction

Fig. 13 shows that sulfated tetragonal zirconia was a better catalyst than sulfated monoclinic zirconia for this reaction. At 6 h reaction time the conversion with the tetragonal catalyst was 94% while with the monoclinic catalyst the maximum conversion was 65%. During the first 2 h of reaction the monoclinic catalyst was noticeably more active but its activity then decreased and disappeared completely after 3 h, the conversion remaining constant thereafter.

The activity results are more possible related to the acidity of the catalysts since sucrose inversion is an acid-catalyzed reaction [30]. More especifically the activity should be related to the Brønsted acidity because for this reaction Brønsted acid sites are more important than the Lewis ones [31]. However, there is no good correlation between the higher surface concentration of acid sites of the tetragonal sample and the lower initial activity of this catalyst.

According to Gehlawat [32], invert sugar is traditionally produced from sucrose using mineral acids like H_2SO_4 or HCl and that this conventional method suffers from low conversion efficiency (65–70%), high ash content and undesirable products (7–8%). The same author reports that complete conversion in 30 min reaction time can be got when reacting sucrose over strong cationic resin beds. Mendes et al. [33] shows that 59% conversion can be got with Amberlite IR 120 resins in packed beds when using a contact time of about 9 min and 70 °C temperature. These reported reaction rate values correspond to 5–6 times the rate observed for the sulfated zirconia catalyst for similar reaction conditions.

3.4.2. Glycerol esterification

Glycerol esterification with fatty acids can be catalyzed by basic and acid catalysts, homogeneous or heterogeneous. Solid acids have lately attracted much interest for this reaction because of the environmental concern associated to mineral strong acids, like H_2SO_4, and because of the convenience for the separation of products and catalyst. Homogeneous acids also have selectivity problems and usually yield a mixture of mono-, di- and triglycerides, when in most cases only the monoglyceride is the desired product. Concerning the use of solid acid catalysts, Abro et al. [34] reacted oleic acid and glycerol using cationic resin catalysts and obtained a selectivity to mono-oleyl glyceride of 90% at a conversion of 50% over the gel resin Amberlyst 31. Machado et al. [35] used zeolitic molecular sieves as catalysts for the synthesis of glycerol monolaurate and reported that the best results were obtained by using zeolite Beta as catalyst, and monolaurate yields of 20% with selectivities higher than 65% were achieved. Wang et al. [36] esterified free fatty acids in biodiesel with glycerol, using SO_4^{2-}–ZrO_2–Al_2O_3 as catalyst. They achieved a stable conversion of 98.4% at 200 °C, a glycerol:fatty acid molar ratio of 1.4 and a reaction time of 4 h.

Fig. 14 shows the results of glycerol esterification using monoclinic and tetragonal sulfated zirconia catalysts. It can be seen that the activity of the monoclinic catalysts is many times higher than that of the tetragonal catalysts. Practically, total conversion is obtained at 4 h of reaction time when the monoclinic sulfated zirconia catalyst is used. At the same reaction time the conversion achieved with the tetragonal sulfated zirconia catalyst is about 30% only.

One possible explanation of the higher activity of the monoclinic sample is its greater concentration of surface Lewis acid sites. Considering the amount of sites measured by pyridine adsorption and FTIR absorption after evacuation at 423 K, monoclinic sulfated zirconia has 51 μmol g^{-1} of Lewis acid sites and 5 μmol g^{-1} of Brønsted acid sites. This yields a Brønsted/Lewis acid ratio of 0.098. Tetragonal sulfated zirconia has 11 μmol g^{-1} of Lewis acid sites and 23 μmol g^{-1} of Brønsted acid sites thus having a Brønsted/Lewis ratio of 2.09. While the evidence of the role of Lewis acid sites in

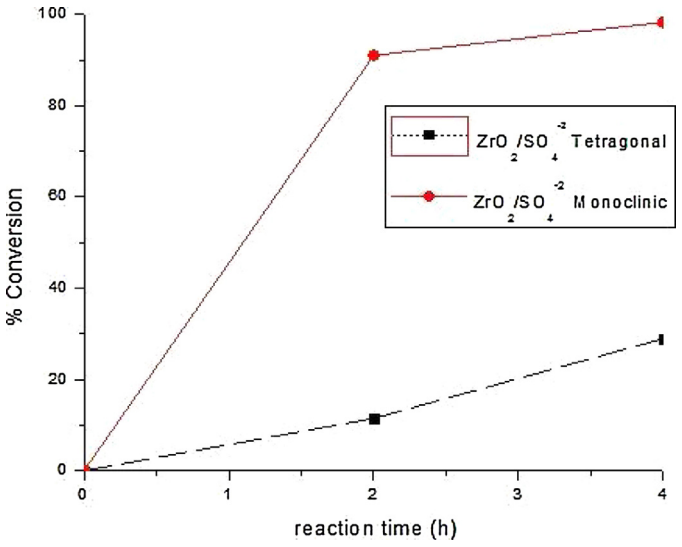

Fig. 14. Results of the glycerol esterification reaction as catalyzed by ZrO_2–SO_4^{2-} catalysts, monoclinic (dashed line) and tetragonal phase (continuous line). Molar ratio of glycerol to fatty acid equal to one; 0.16 g of catalyst; stirred at 800 rpm; temperature: 100 °C.Time of reaction: 4 h.

Table 4
Catalytic activity of sulfated zirconia catalysts in the reaction of glycerol esterification with lauric acid. Molar ratio of glycerol to fatty acid equal to one; 0.16 g of catalyst; stirred at 800 rpm; temperature: 100 °C. Time of reaction: 4 h.

Catalyst	$\frac{\text{moles of lauric acid}}{h \times \text{mmol H+/gcatalyst}}$
ZrO_2–SO_4^{2-} Monoclinic	4.5×10^{-2}
ZrO_2–SO_4^{2-} Tetragonal	2.0×10^{-2}

glycerol esterification seems to be scarce, some authors claim that water tolerant $SnCl_2$ having only Lewis acid sites could catalyze the formation of glycerol acetates with great yield (Goncalves et al. [37]).

If active sites on monoclinic sulfated zirconia are responsible for the catalytic activity then it must be considered that the water in the reaction medium can be a poison of the activity. It is well known that acid catalysts for esterification of fatty acids are deactivated during the reaction because of the formation of water (Yan et al. [38]). Water hydrates surface proton and decreases its surface strength and can also transform Lewis sites into Brønsted ones. In this sense the deactivation seen for the monoclinic catalyst during the inverse sucrose reaction, could be a consequence of the presence of water in the medium. No deactivation was however seen in the case of the reaction of glycerol transesterification. In this case the water formed as a product of the esterification could have escaped from the reaction medium, since the reaction temperature was 100 °C and the reactor was an open glass flask Table 4.

A comparison of the results on both reactions indicates that activity was higher for monoclinic zirconia in esterification of glycerol and higher for tetragonal zirconia in sucrose inversion. Both are acid-catalyzed reactions and both catalysts had surfaces with acid sites of similar strength. The total acidity (per unit mass) was higher for monoclinic zirconia while the surface density of acid sites (in mmol m^{-2}) was higher for tetragonal zirconia. Sulfated monoclinic zirconia had mainly Lewis acid sites while tetragonal zirconia mainly Brønsted ones. In this sense the results could be related to glycerol esterification being catalyzed mainly by isolated sites of any kind (thus being more favored on monoclinic zirconia that had more acid sites) and sucrose inversion being catalyzed mainly by Brønsted acid sites.

4. Conclusions

Monoclinic and tetragonal sulfated zirconia catalysts with only one crystal phase were synthesized by means of the sulfation of crystalline supports previously obtained by controlled precipitation and calcination. The use of crystalline samples yielded final catalysts with low specific surface area that however showed good activity in the reaction tests. Compared to ion exchange resin catalysts sulfated zirconia catalysts had a similar reaction rate in the reaction of glycerol esterification and a lower one (1/5–1/6) in the reaction of sucrose inversion.

FTIR characterization indicated that both monoclinic and tetragonal catalysts had surface sulfate groups with a bridge structure. Sulfate addition greatly increased the acidity and also promoted the appearance of Brønsted acid sites, in comparison to the base unsulfated supports that only had a moderate concentration of Lewis sites.

On a mass basis the monoclinic sulfated zirconia catalyst had a higher amount of acid sites, as measured either by pyridine adsorption or by the Hammett indicator method.

The catalysts were used in the reaction of sucrose inversion and glycerol esterification with lauric acid. The initial reaction rate was higher on the monoclinic catalyst in both reactions, but the activity was decreased after a few hours in the case of the sucrose inversion reaction. The activity of the tetragonal catalyst was stable in both reactions and total conversion of sucrose was obtained after a few hours reaction time.

The activity of the monoclinic catalysts seems to be mainly related to the presence of Lewis acid sites. Deactivation by water could be the reason for the activity drop in the case of the sucrose reaction. Continuous water evaporation at the reaction conditions could be responsible for the stable performance of this catalyst in the case of the esterification reaction.

Acknowledgements

The authors are grateful to University of Cauca for the financial support given to this research. Special thanks to the LUMILAB laboratory of Universiteit Gent (Belgium) and the Université de Poitiers (France) for their collaboration with the XPS spectra and X-ray diffractograms, respectively.

References

[1] B. Reddy, P. Sreekanth, P. Lakshmanan, J. Mol. Catal. A: Chem. 237 (2005) 93–100.
[2] G. Yadav, G. Pathre, Microporous Mesoporous Mat. 89 (2006) 16–24.
[3] M. Ecormier, K. Wilson, A. Lee, J. Catal. 215 (2003) 57–65.
[4] B. Reddy, M. Patil, B. Reddy, S. Park, Catal. Commun. 9 (2008) 950–954.
[5] R. Srinivasan, Catal. Lett. 14 (1992) 165–170.
[6] A. Zarubica, P. Putanov, G. Boskovic, J. Serb. Chem. Soc. 72 (2007) 679–686.
[7] B. Reddy, M. Patil, B. Redd, Catal.Lett. 126 (2008) 413–418.
[8] M. Ropot, E. Angelescu, R. Zăvoianu, R. Bîrjeg, Rev. Chim. 59 (2008) 292–296.
[9] C.R. Vera, C. Pieck, K. Shimizu, J. Parera, Appl. Catal. A: Gen. 230 (2002) 137–151.
[10] R. Comelli, C. Vera, J. Parera, J. Catal. 151 (1996) 96–101.
[11] R. Srinivas, D. Taulbee, H.D. Burtron, Catal. Lett. 9 (1991) 1–7.
[12] D. Tichit, B. Coq, H. Armendariz, F. Figuéras, Catal.Lett. 1 (1996) 109–113.
[13] C. Morterra, G. Cerrato, F. Pinna, M. Signoretto, J. Catal. 157 (1995) 109–123.
[14] Y. Sun, L. Yuan, W. Wang, C. Chen, F. Xiao, Catal. Lett. 87 (2003) 57–61.
[15] W. Stichert, F. Schüth, S. Kuba, H. Knözinger, J. Catal. 198 (2001) 277–285.
[16] G. Yadav, J. Nair, Microporous and Mesoporous Mat. 33 (1999) 1–48.
[17] T. Yamaguchi, Appl. Catal. 6 (1990) 1–25.
[18] J.E. Rodríguez, D. Campo, DYNA 165 (2011) 224–233.
[19] D. Milburn, K. Saito, R. Keogh, B. Davis, Appl. Catal. A: Gen. 215 (2001) 191–197.
[20] F. Babou, G. Coudurier, J. Vedrine, J. Catal. 153 (1995) 341–349.
[21] M. Cattania, S. Ardizzone, C. Bianchi, S. Carella, Colloid Surf. Physicochem. Eng. Aspect 76 (1993) 233–240.
[22] S. Ardizzone, C. Bianchi, E. Grassi, Colloids Surf. 135 (1998) 41–51.
[23] S. Ardizzone, C. Bianchi, Appl. Surf. Sci. 152 (1999) 63–69.
[24] V. Pârvulescu, S. Coman, P. Grange, Appl. Catal. A: Gen. 176 (1999) 27–43.

[25] P.S. Querino, J.R. Bispo, M. Rangel, Catal. Today 107–108 (2005) 920–925.
[26] J. Shackelford, R. Doremus, Ceramic and Glass Materials: Structure Properties and Processing, Springer-Verlag, Gremany, 2008.
[27] B.M. Reddy, M.K. Patil, B.T. Reddy, Catal. Lett. 126 (2008) 413–418.
[28] Busto, et al., App. Catal. A: Gen 348 (2) (2014) 173–182.
[29] M. Yurdakoc, M. Akcay, Y. Tonbul, K. Yurdakoc, Turk. J. Chem. 23 (1999) 319–327.
[30] Paul M. Leininger, M. Kilpatrick, J. Am. Chem. Soc. 60 (12) (1938) 2891–2899.
[31] S. Sumiya, T. Oumi, Y. Sadakane, M. Sano, Appl. Catal. A: Gen. 365 (2) (2009) 261–267.
[32] J. Gehlawat, Indian J. Chem. Technol. 8 (2001) 28–32.
[33] Mendes, et al., Int. J. Engng Ed. 19 (2003) 893–901.
[34] Abro, et al., Stud. Surf. Sci. 108 (1997) 539–546, Catal.
[35] Machado, et al., Appl. Catal. A 203 (2000) 321–328.
[36] Wang, et al., Eur. J. Lipid Sci. Technol. 114 (2012) 315–324.
[37] Goncalves, et al., Catal. Lett. 141 (2011) 1111–1117.
[38] Yan, et al., App. Catal. A: Gen 353 (2009) 203–212.